

中国格点QCD第一届年会

2021.10.31

Finite-volume and finite-temperature effects
in chiral effective field theory



郭志辉

东南大学

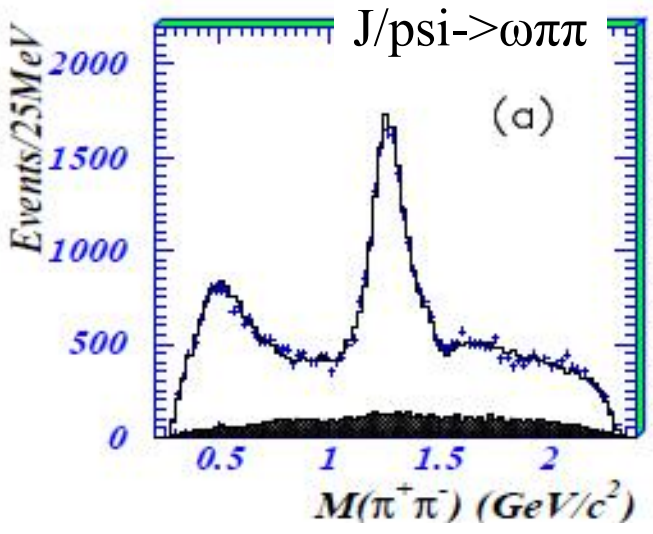
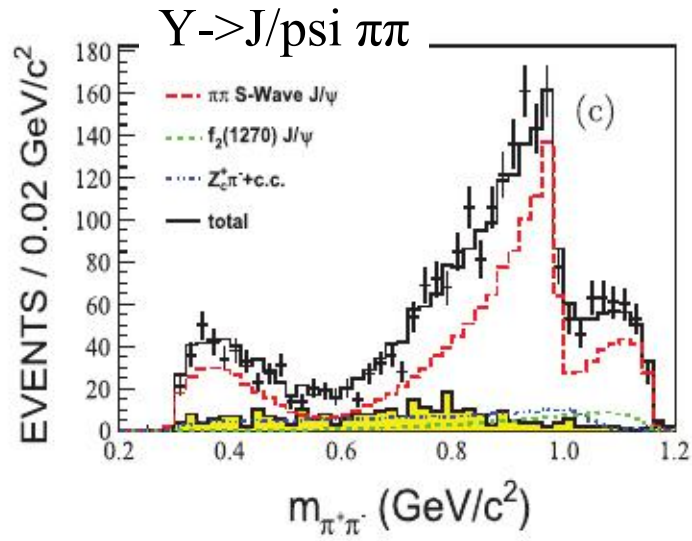
Outline:

1. Introduction
2. Chiral EFT in finite box and its application in lattice
3. Hints of chiral symmetry restoration: scalar resonances at finite temperatures
4. Conclusions

Introduction

Scattering: an important approach to study hadron resonances

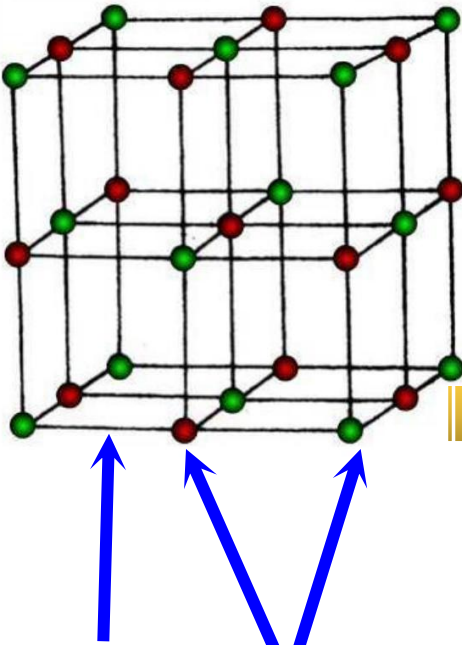
Line shapes for the same resonance can be quite different in different channels.



In contrast, resonance poles of scattering amplitudes are **universal** in all the channels. Different line shapes can be explained by different residues/couplings.

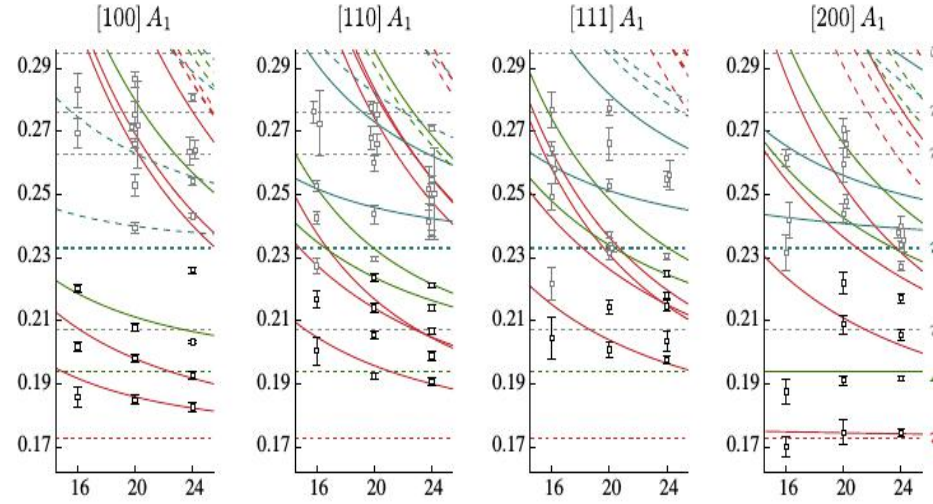
However it is rather challenging to extract scattering observables directly from Exp.

Lattice QCD provides a unique way for this problem !



Significant progress on meson-meson scattering in lattice simulation

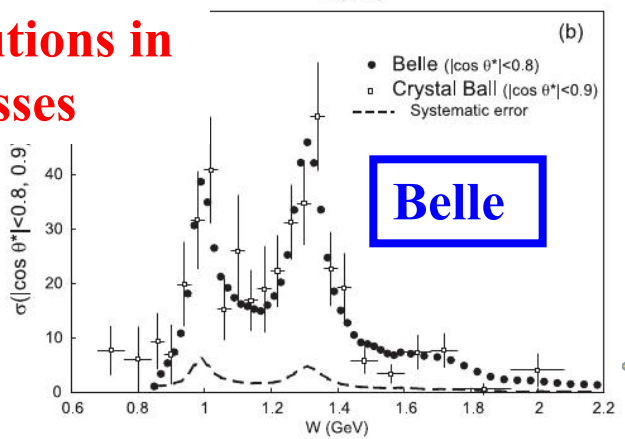
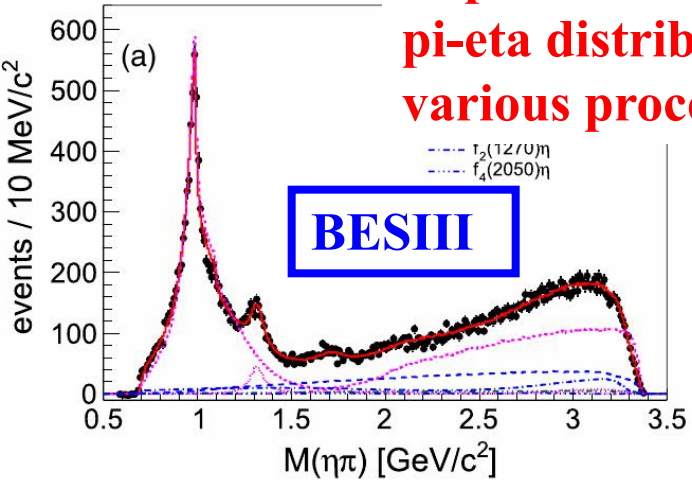
E.g. π - η , $K\bar{K}$, π - η' scattering
 [Dudek, Edwards, Wilson, PRD'16]



Gluon Quark

Data "measured" by lattice: finite-volume energy levels

Exp measurement of π - η distributions in various processes



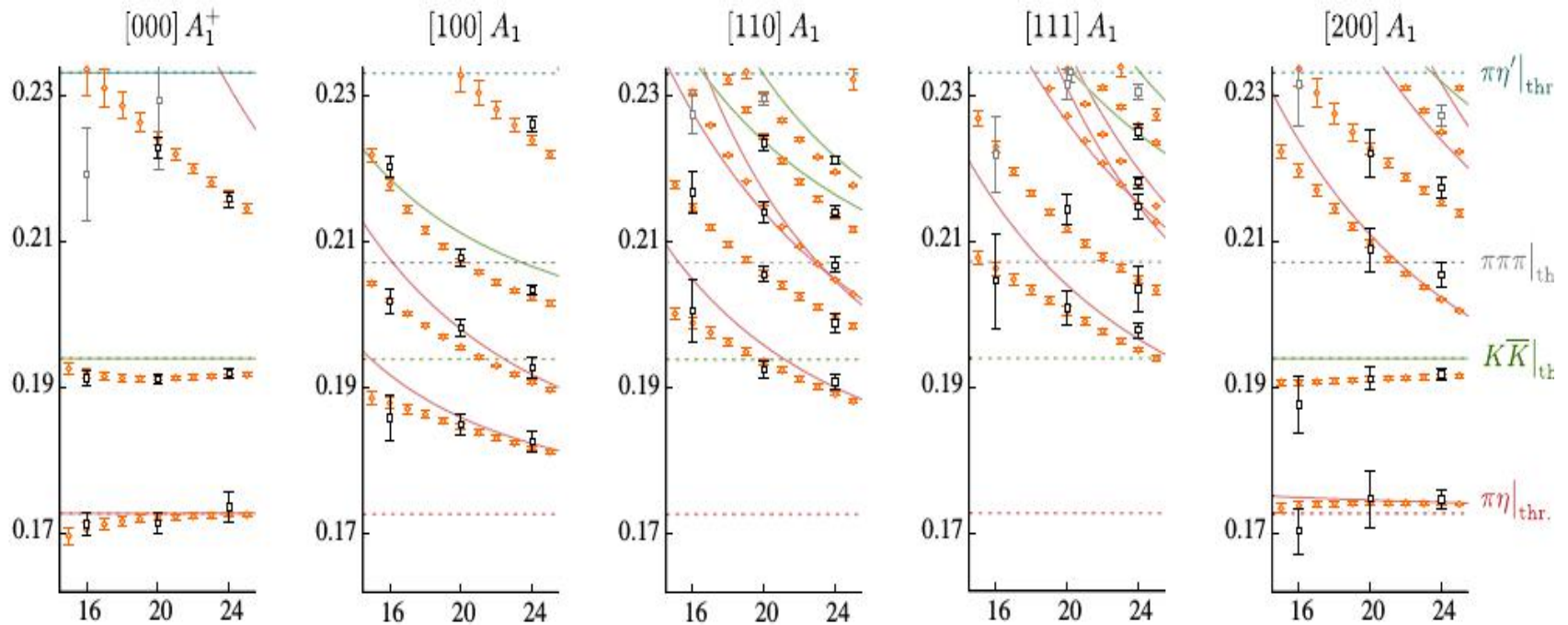
Physical Scattering Amplitudes

First Lattice calculation on coupled-channel pi-eta, KKbar

[Dudek, Edwards, Wilson, PRD'16]

$$m_\pi = 390 \text{ MeV}$$

Eigenenergies in finite box



Length of finite box

[He, Feng, Liu, JHEP'05] [Wilson, Briceno, Dudek, Edwards, Thomas, PRD '15]

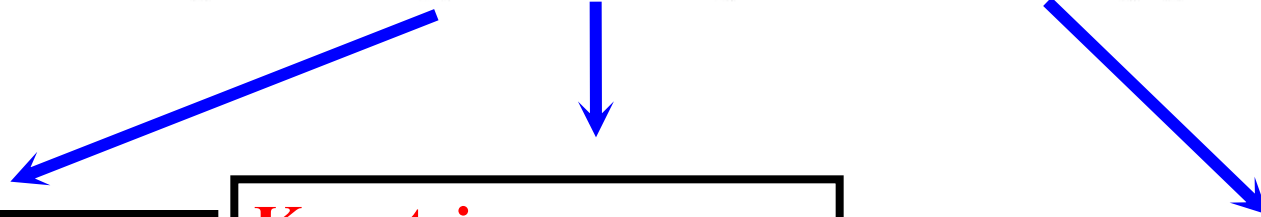
[Lang, Leskovec, Mohler, Prelovsek, Woloshyn, PRD'14] [Fu, PRD'12]

[Gockeler, Horsley, Lage, Meissner, Rakow, Rusetksy, Schierholz, Zanotti, PRD'12]

A widely used approach in the inelastic scattering case:

Luscher function + K matrix

$$\det[\mathbf{1} + i\rho \cdot \mathbf{t} \cdot (\mathbf{1} + i\mathcal{M})] = 0$$



Kinematical factor

K matrix:
polynomial + pole terms

Luscher's finite-volume functions (complex objects)

- Free parameters in K matrix are determined by the finite-volume spectra. Then one can determine amplitudes in infinite volume.
- K matrix does not automatically respect the QCD symmetries, such as the chiral symmetry. It could be problematic for chiral extrapolation.

Chiral approach + Luscher formula:

Step 1: Put chiral perturbation theory (ChPT) in finite volume.

Step 2: The free parameters in ChPT, which are independent of quark masses and volumes, are fitted to the finite-volume energy levels obtained at (un)physical quark masses.

Step 3: Perform the chiral extrapolation and give the predictions in infinite volume with physical quark masses, including phase shifts, inelasticities, resonance poles, etc.

Step 4: Proceed with the standard routine of hadron phenomenologies by taking the physical amplitudes determined from Lattice QCD.

Chiral amplitudes in finite box

Finite-volume effects in scattering process

Two types of finite volume dependence of scattering amplitudes:

- Exponentially suppressed type $\propto \exp(-m_p L)$: ***s, t, u* channels**
- Power suppressed type $\propto 1/L^3$: ***only s* channel**

Current lattice calculations usually take big enough volume L , and therefore one could neglect the exponentially suppressed terms, indicating that finite-volume effects only enter through *s* channel.

Prescription: Algebraic approximation of N/D (a variant version of K-matrix)

$$T_J(s) = \frac{N(s)}{1 + G(s) N(s)}$$

- **The s-channel unitarity is exact. The crossed-channel dynamics is included in a perturbative manner.**

- **Unitarity condition:** $\text{Im}G(s) = -\rho(s)$

$$G(s) = \boxed{a^{SL}(s_0)} - \frac{s - s_0}{\pi} \int_{4m^2}^{\infty} \frac{\rho(s')}{(s' - s)(s' - s_0)} ds'$$

Finite-volume effects enter via $G(s)$

- **$N(s)$: crossed-channel contributions of partial-wave amplitudes from chiral EFT. Finite-volume effects are suppressed for $N(s)$.**

Finite-volume effects in s-channel unitarity function $G(s)$

$$G(s) = i \int \frac{d^4 q}{(2\pi)^4} \frac{1}{(q^2 - m_1^2 + i\epsilon)[(P - q)^2 - m_2^2 + i\epsilon]}, \quad s \equiv P^2$$

Sharp momentum cutoff to regularize $G(s)$

$$G(s)^{\text{cutoff}} = \int^{|\vec{q}| < q_{\text{max}}} \frac{d^3 \vec{q}}{(2\pi)^3} I(|\vec{q}|), \quad \begin{aligned} I(|\vec{q}|) &= \frac{w_1 + w_2}{2w_1 w_2 [E^2 - (w_1 + w_2)^2]}, \\ w_i &= \sqrt{|\vec{q}|^2 + m_i^2}, \quad s = E^2 \end{aligned}$$

$G(s)$ in a finite box of length L with periodic boundary condition

$$\tilde{G} = \frac{1}{L^3} \sum_{\vec{n}}^{|\vec{q}| < q_{\text{max}}} I(|\vec{q}|), \quad \vec{q} = \frac{2\pi}{L} \vec{n}, \quad \vec{n} \in \mathbb{Z}^3$$

Finite-volume correction ΔG

[Doring, Meissner, Oset, Rusetsky, EPJA11]

$$\begin{aligned} \Delta G &= \tilde{G} - G^{\text{cutoff}} \\ &= \left\{ \frac{1}{L^3} \sum_{\vec{q}}^{|\vec{q}| < q_{\text{max}}} - \int^{|\vec{q}| < q_{\text{max}}} \frac{d^3 \vec{q}}{(2\pi)^3} \right\} \frac{1}{2\omega_1(\vec{q}) \omega_2(\vec{q})} \frac{\omega_1(\vec{q}) + \omega_2(\vec{q})}{E^2 - (\omega_1(\vec{q}) + \omega_2(\vec{q}))^2} \end{aligned}$$

Finite-volume effects in the moving frames

Lorentz invariance is lost in finite box. One needs to work out the explicit form of the loops when boosting from one frame to another.

transforming $\vec{q}_{i=1,2}$ to $\vec{q}_{i=1,2}^*$ \longrightarrow **CM quantities**

$$\vec{q}_i^* = \vec{q}_i + \left[\left(\frac{P^0}{E} - 1 \right) \frac{\vec{q}_i \cdot \vec{P}}{|\vec{P}|^2} - \frac{q_i^0}{E} \right] \vec{P}$$

moving frame with total four-momentum $P^\mu = (P^0, \vec{P})$ $s = E^2 = (P^0)^2 - |\vec{P}|^2$

Impose on-shell condition

$$q_i^{*0} = \sqrt{|\vec{q}_i^*|^2 + m_i^2}$$

$$q_i^0 = \frac{q_i^{*0} E + \vec{q}_i \cdot \vec{P}}{P^0} \longrightarrow q_i^0 = \sqrt{|\vec{q}_i|^2 + m_i^2}$$

G function in the moving frame

$$\int_{|\vec{q}_1|^* < q_{\max}} \frac{d^3 \vec{q}_1^*}{(2\pi)^3} I(|\vec{q}_1^*|) \implies \tilde{G}^{\text{MV}} = \frac{E}{P^0 L^3} \sum_{\vec{q}_1}^{|\vec{q}_1^*| < q_{\max}} I(|\vec{q}_1^*(\vec{q}_1)|) \quad \begin{aligned} \vec{q}_1 &= \frac{2\pi}{L} \vec{n}, & \vec{n} &\in \mathbb{Z}^3, \\ \vec{P} &= \frac{2\pi}{L} \vec{N}, & \vec{N} &\in \mathbb{Z}^3 \end{aligned}$$

Finite-volume correction ΔG^{MV} :

$$\Delta G^{\text{MV}} = \tilde{G}^{\text{MV}} - G^{\text{cutoff}}$$

Mixing of different partial waves in finite volume

The mixing between different partial waves is absent in the infinite volume:

$$\int_0^{2\pi} d\phi \int_0^\pi \sin\theta d\theta Y_{\ell m}(\theta, \phi) Y_{\ell' m'}^*(\theta, \phi) = \delta_{\ell\ell'} \delta_{mm'}$$

The mixing appears in finite-volume case, due to the absence of the general orthogonal conditions of spherical harmonic functions.

The mixing patterns vary in different irreducible representations and different moving frames.

$$\det[\mathbf{1} + i\rho \cdot \mathbf{t} \cdot (\mathbf{1} + i\mathcal{M})] = 0$$

[He, Feng, Liu, JHEP'05] [Wilson, Briceno, Dudek, Edwards, Thomas, PRD '15]

[Lang, Leskovec, Mohler, Prelovsek, Woloshyn, PRD'14] [Fu, PRD'12]

[Gockeler, Horsley, Lage, Meissner, Rakow, Rusetksy, Schierholz, Zanotti, PRD'12]

We adapt the following approach to proceed the study of unitarized ChpT in finite volume.

[Gockeler, Horsley, Lage, Meissner, Rakow, Rusetksy, Schierholz, Zanotti, PRD'12]

Finite-volume correction to G function:

$$\Delta G_{\ell m}^{\text{MV}} = \tilde{G}_{\ell m}^{\text{MV}} - G^{\text{cutoff}} \delta_{\ell 0} \delta_{m 0}$$

$$\tilde{G}_{\ell m}^{\text{MV}} = \sqrt{\frac{4\pi}{2\ell + 1}} \frac{1}{L^3} \frac{E}{P^0} \sum_{\vec{n}}^{|\vec{q}^*| < q_{\text{max}}} \left(\frac{|\vec{q}^*|}{|\vec{q}^{\text{on}*}|} \right)^\ell Y_{\ell m}(\hat{q}^*) I(|\vec{q}^*|)$$

It is equivalent to the $w_{\ell m}$ function, up to exponentially suppressed terms [Gockeler, Horsley, Lage, et al., PRD'12]

$$w_{\ell m} = \frac{1}{\pi^{3/2} \sqrt{2\ell + 1}} \gamma^{-1} q^{-\ell-1} Z_{\ell m}^\Delta(1, q^2)$$

$$Z_{js}^\Delta(\delta, q^2) = \sum_{z \in P_\Delta} \frac{y_{js}(z)}{(z^2 - q^2)^\delta}$$

$$y_{\ell m}(\mathbf{r}) = |\mathbf{r}|^\ell Y_{\ell m}(\hat{\mathbf{r}}), \quad \hat{\mathbf{r}} = \frac{\mathbf{r}}{|\mathbf{r}|}$$

$$\tilde{G}_{\ell m}^{\text{MV}} = -\frac{|\vec{q}^{\text{on}*}|}{8\pi E} w_{\ell m}$$

Final expression for the G function:

$$\tilde{G}_{\ell m}^{\text{MV}} = G^{V\infty} \delta_{\ell 0} \delta_{m 0} + \Delta G_{\ell m}^{\text{MV}}$$

Example: when only S and P waves are included.

$$\mathbf{A}_1^+ (0,0,0) : \quad \det[1 + N_0(s) \cdot \tilde{G}_{00}] = 0$$

$$\mathbf{T}_1^- (0,0,0) : \quad \det[1 + N_1(s) \cdot \tilde{G}_{00}] = 0$$

$$\mathbf{A}_1 (0,0,1) : \quad \det[I + N_{0,1} \cdot \mathcal{M}_{0,1}^{A_1}] = 0 ,$$

$$N_{0,1} = \begin{pmatrix} N_0 & 0 \\ 0 & N_1 \end{pmatrix} , \quad \mathcal{M}_{0,1}^{A_1} = \begin{pmatrix} \tilde{G}_{00} & i\sqrt{3}\tilde{G}_{10} \\ -i\sqrt{3}\tilde{G}_{10} & \tilde{G}_{00} + 2\tilde{G}_{20} \end{pmatrix}$$

$$N_{0,1} \cdot \mathcal{M}_{0,1}^{A_1} = \begin{pmatrix} N_{0,11}\tilde{G}_{00,1} & N_{0,12}\tilde{G}_{00,2} & N_{0,13}\tilde{G}_{00,3} & i\sqrt{3}N_{0,11}\tilde{G}_{10,1} \\ N_{0,21}\tilde{G}_{00,1} & N_{0,22}\tilde{G}_{00,2} & N_{0,23}\tilde{G}_{00,3} & i\sqrt{3}N_{0,21}\tilde{G}_{10,1} \\ N_{0,31}\tilde{G}_{00,1} & N_{0,32}\tilde{G}_{00,2} & N_{0,33}\tilde{G}_{00,3} & i\sqrt{3}N_{0,31}\tilde{G}_{10,1} \\ -i\sqrt{3}N_1\tilde{G}_{00,1} & 0 & 0 & N_1(\tilde{G}_{00,1} + 2\tilde{G}_{20,1}) \end{pmatrix}$$

[ZHG,Liu,Meissner,Oller,Rusetsky, EPJC'19]

**Several applications in analyzing the lattice
finite-volume energy levels**

$\pi\eta$, $KK\bar{K}$, $\pi\eta'$ coupled-channel system and $a_0(980)$

Leading order amplitudes from U(3) ChPT:

$$T_{J=0}^{I=1, \pi\eta \rightarrow \pi\eta}(s)^{(2)} = \frac{(c_\theta - \sqrt{2}s\theta)^2 m_\pi^2}{3F_\pi^2},$$

$$T_{J=0}^{I=1, \pi\eta \rightarrow K\bar{K}}(s)^{(2)} = \frac{c_\theta(3m_\eta^2 + 8m_K^2 + m_\pi^2 - 9s) + 2\sqrt{2}s\theta(2m_K^2 + m_\pi^2)}{6\sqrt{6}F_\pi^2},$$

$$T_{J=0}^{I=1, \pi\eta \rightarrow \pi\eta'}(s)^{(2)} = \frac{(\sqrt{2}c_\theta^2 - c_\theta s\theta - \sqrt{2}s\theta^2)m_\pi^2}{3F_\pi^2},$$

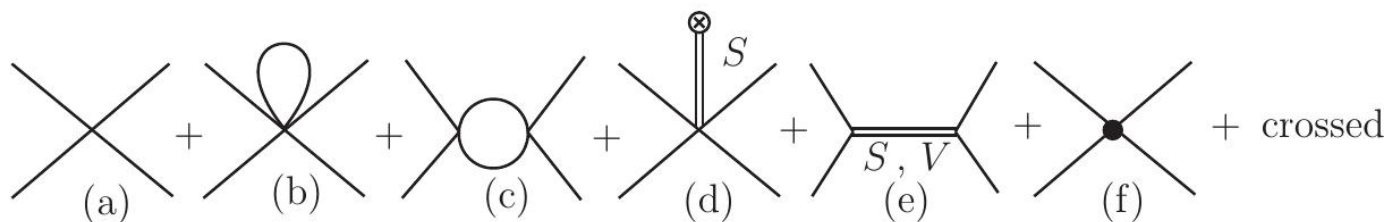
$$T_{J=0}^{I=1, K\bar{K} \rightarrow K\bar{K}}(s)^{(2)} = \frac{s}{4F_\pi^2},$$

$$T_{J=0}^{I=1, K\bar{K} \rightarrow \pi\eta'}(s)^{(2)} = \frac{s\theta(3m_{\eta'}^2 + 8m_K^2 + m_\pi^2 - 9s) - 2\sqrt{2}c_\theta(2m_K^2 + m_\pi^2)}{6\sqrt{6}F_\pi^2},$$

$$T_{J=0}^{I=1, \pi\eta' \rightarrow \pi\eta'}(s)^{(2)} = \frac{(\sqrt{2}c_\theta + s\theta)^2 m_\pi^2}{3F_\pi^2},$$

Higher-order amplitudes are also explored

Scattering amplitude :



$\pi\eta$, $KK\bar{K}$, $\pi\eta'$ coupled-channel system and $a_0(980)$

Other inputs to fit the lattice data:

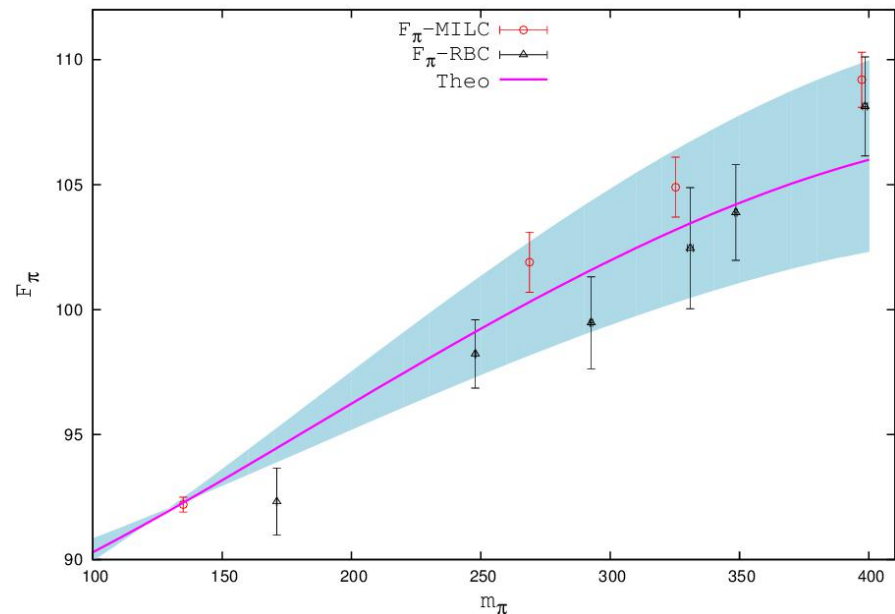
$$m_\pi = 391.3 \pm 0.7 \text{ MeV}, \quad m_K = 549.5 \pm 0.5 \text{ MeV}, \quad m_\eta = 587.2 \pm 1.1 \text{ MeV}, \quad m_{\eta'} = 929.8 \pm 5.7 \text{ MeV}$$

Our estimate of the leading order η - η' mixing angle at unphysical masses

$$\theta = (-10.0 \pm 0.1)^\circ \quad (\theta^{\text{phys}} = -16.2^\circ)$$

We also need to estimate F_π at the unphysical meson masses.

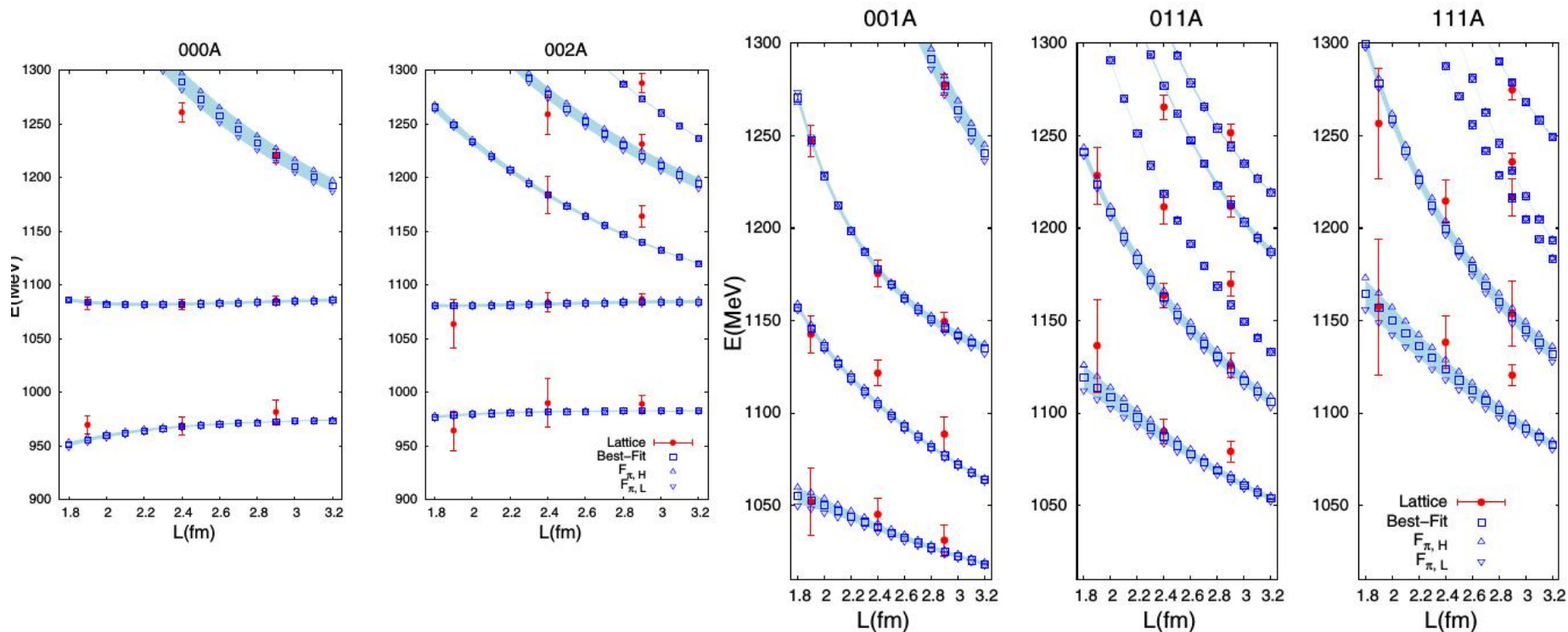
$$F_\pi = F \left\{ 1 - \frac{1}{16\pi^2 F^2} \left[m_\pi^2 \ln \frac{m_\pi^2}{\mu^2} + \frac{m_K^2}{2} \ln \frac{m_K^2}{\mu^2} \right] \right. \\ \left. + \left[\frac{4\tilde{c}_d \tilde{c}_m (m_\pi^2 + 2m_K^2)}{F^2 M_{S_1}^2} - \frac{8c_d c_m (m_K^2 - m_\pi^2)}{3F^2 M_{S_8}^2} \right] \right\}$$



$\pi\eta$, $KK\bar{b}$, $\pi\eta'$ coupled-channel system and $a_0(980)$

Leading order Fit (Only LO amplitudes are included in the $N(s)$ function.)

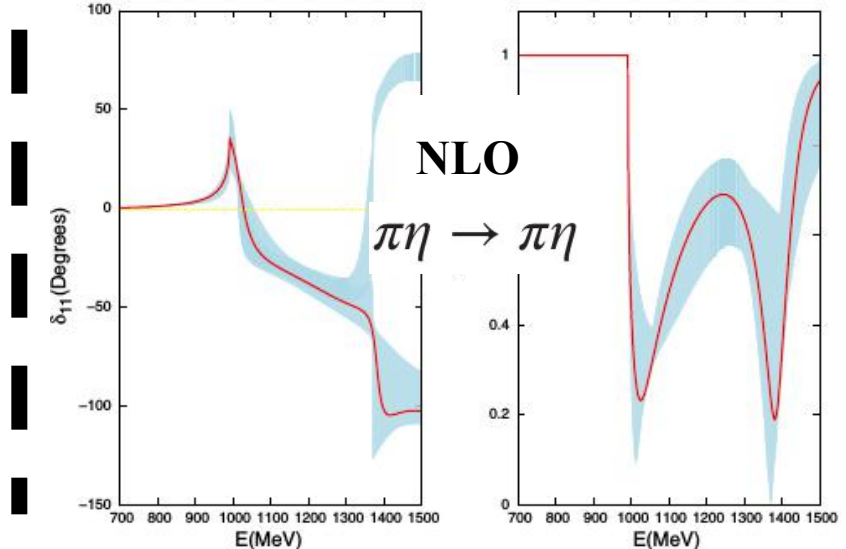
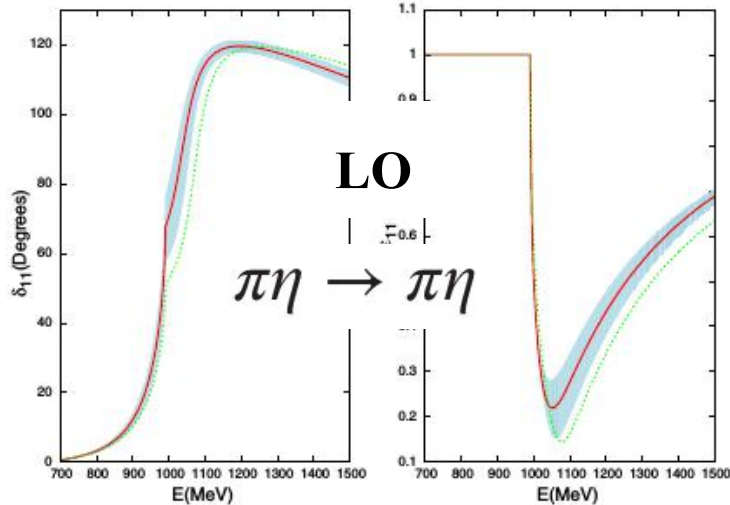
[ZHG, Liu, Meissner, Oller, Rusetsky, PRD'17]



➤ Remark: there is only one free parameter in the fits, i.e. the common subtraction constant !

➤ The quality of NLO fit is quite similar to the LO case.

Phase shifts and inelasticities at physical meson masses

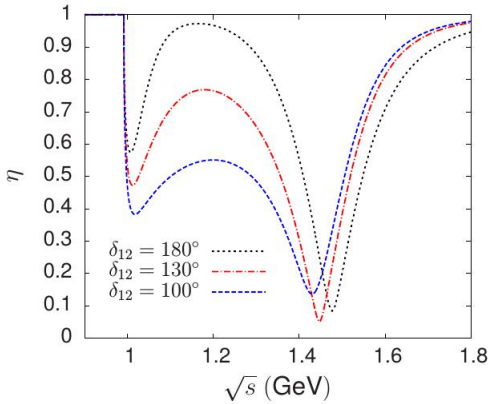
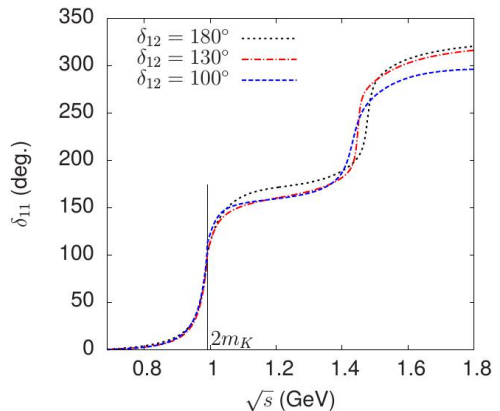


Pole positions and residues of $a_0(980)$ at physical meson masses

Resonance	RS	Mass (MeV)	Width/2 (MeV)	Residue $_{\pi\eta}^{1/2}$ (GeV)	Ratios
LO					
$a_0(980)$	II	1037^{+17}_{-14}	44^{+6}_{-9}	$3.8^{+0.3}_{-0.2}$	$1.43^{+0.03}_{-0.03}$ ($K\bar{K}/\pi\eta$) $0.05^{+0.01}_{-0.01}$ ($\pi\eta'/\pi\eta$)
NLO					
$a_0(980)$	IV	1019^{+22}_{-8}	24^{+57}_{-17}	$2.8^{+1.4}_{-0.6}$	$1.8^{+0.1}_{-0.3}$ ($K\bar{K}/\pi\eta$) $0.01^{+0.06}_{-0.01}$ ($\pi\eta'/\pi\eta$)
$a_0(1450)$	V	1397^{+40}_{-27}	62^{+79}_{-8}	$1.7^{+0.3}_{-0.4}$	$1.4^{+2.4}_{-0.6}$ ($K\bar{K}/\pi\eta$) $0.9^{+0.8}_{-0.2}$ ($\pi\eta'/\pi\eta$)

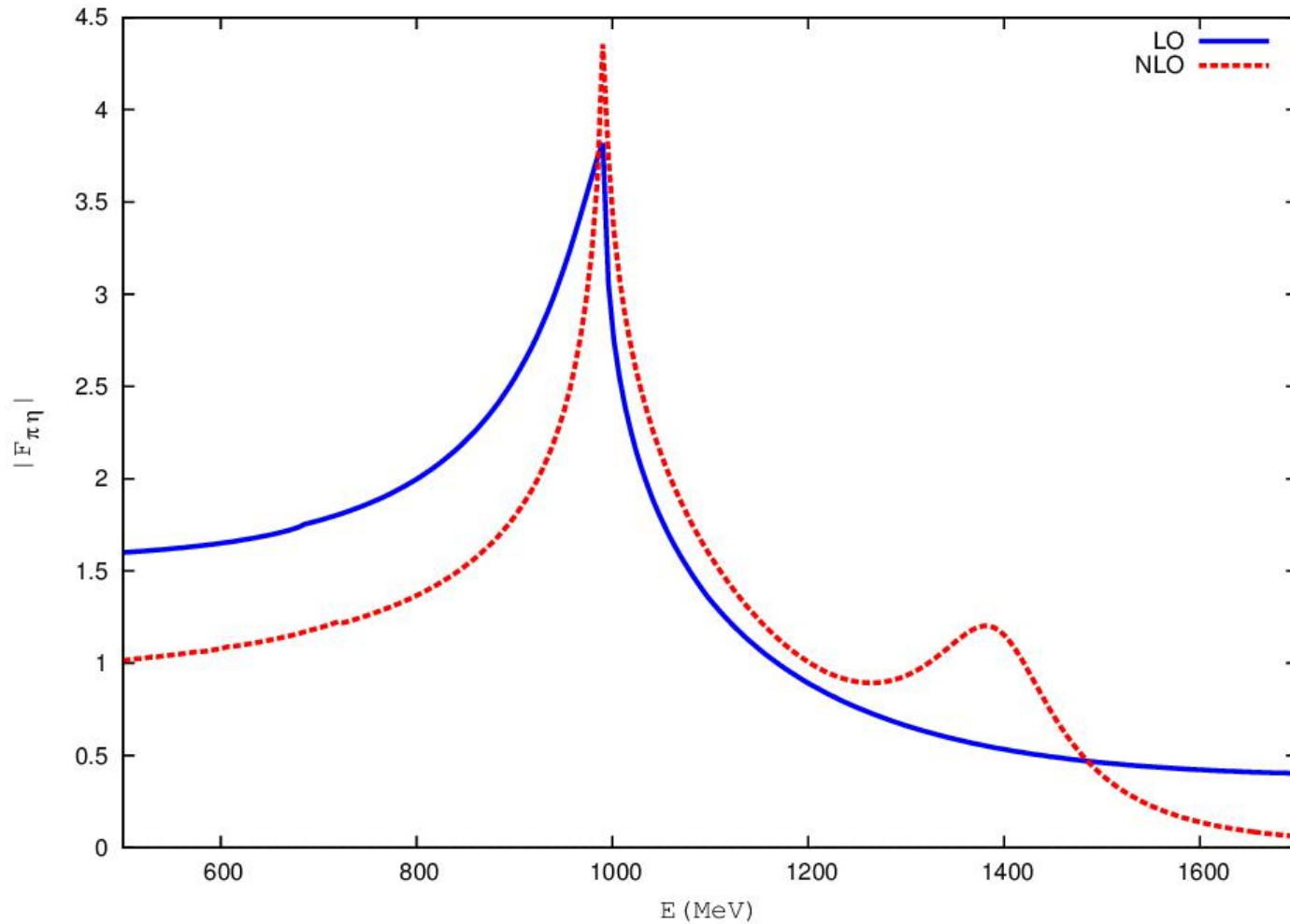
Comparison with the results from another group

[Albaladejo, Moussallam, EPJC'17]



Prediction of the pi-eta scalar form factors

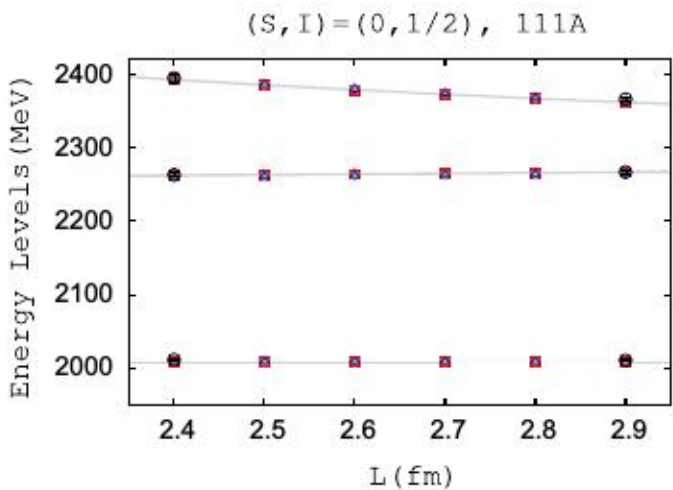
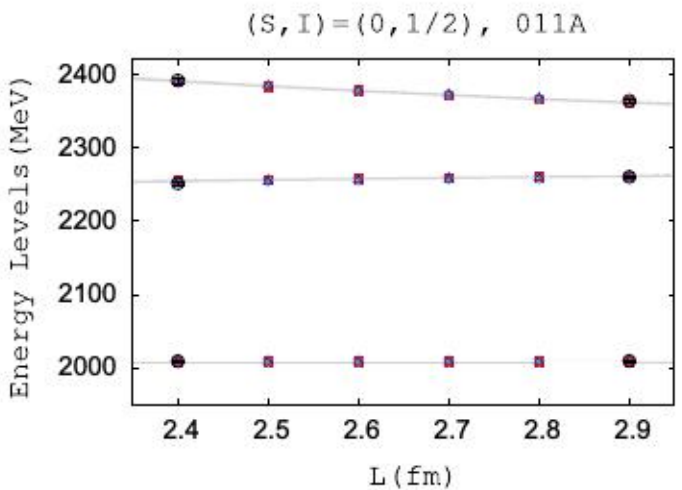
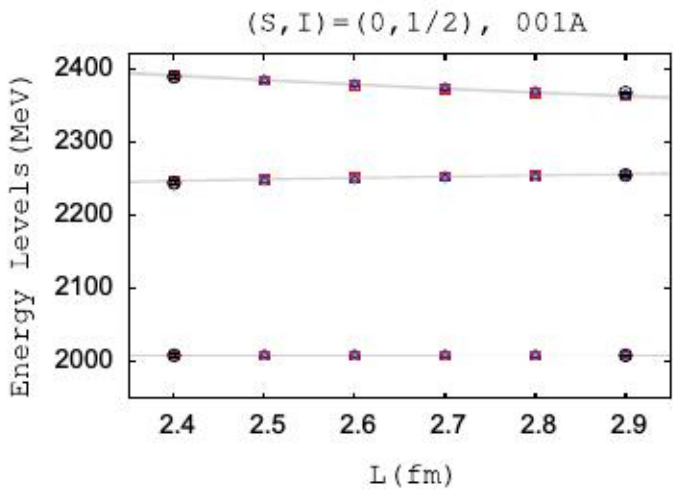
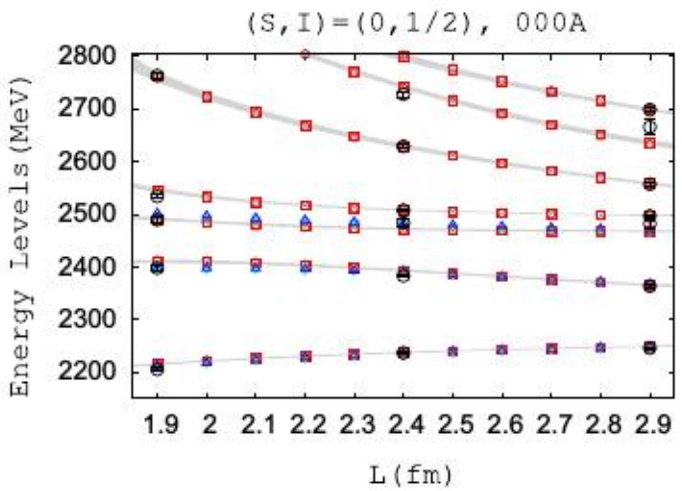
$$F^I(s) = [1 + N^{IJ}(s)g^{IJ}(s)]^{-1}R^I(s)$$



D-pi, D-eta, Ds-Kbar scattering and D*(2400)

Reproduction of the finite-volume energy levels

[Moir,Peardon,Ryan,Thomas,Wilson, JHEP'16]



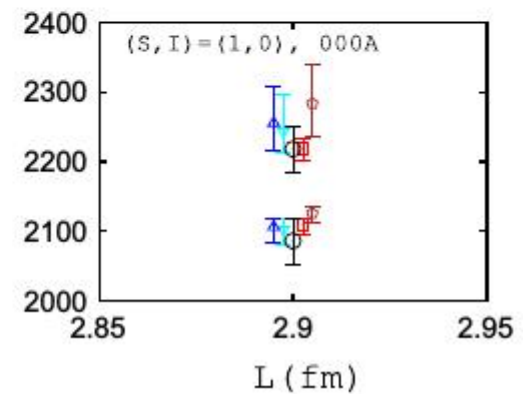
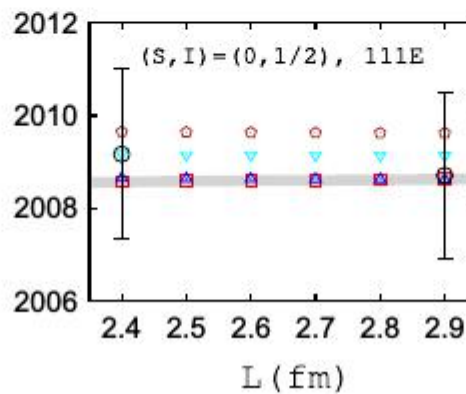
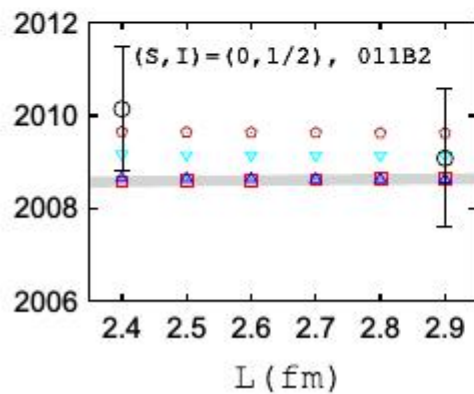
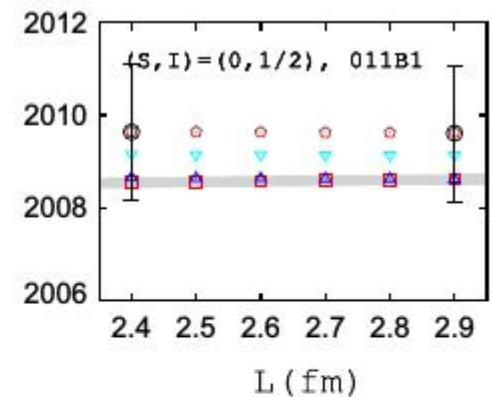
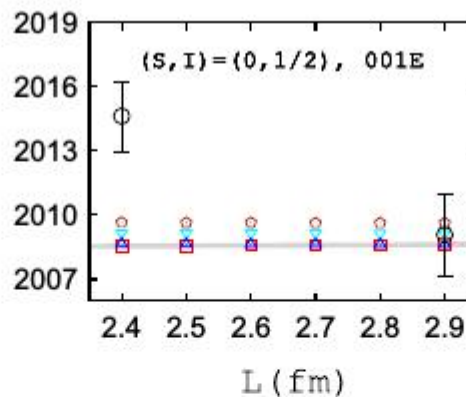
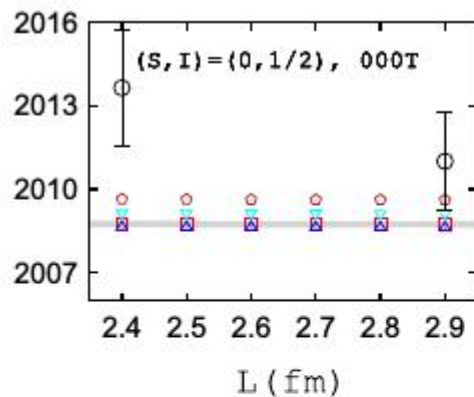
[ZHG,Liu,Meissner,Oller,Rusetsky, EPJC'19]

D-pi, D-eta, Ds-Kbar scattering and $D^*(2400)$

Reproduction of the finite-volume energy levels

[Moir,Peardon,Ryan,Thomas, Wilson, JHEP'16]

[Lang,Leskovec,Mohler,Prelovsek,Woloshyn,PRD'14]

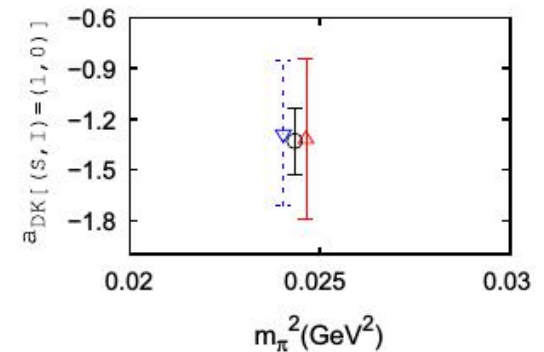
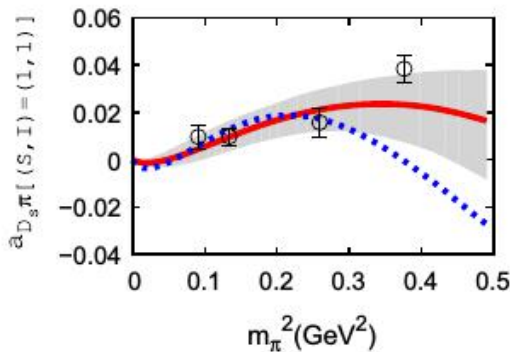
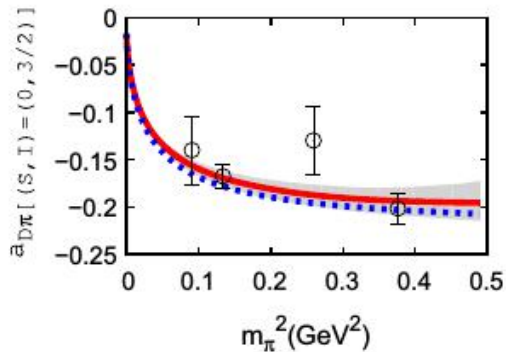
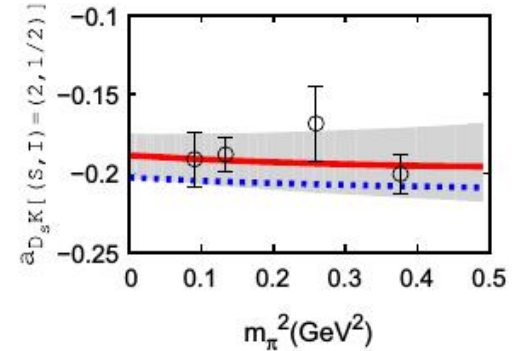
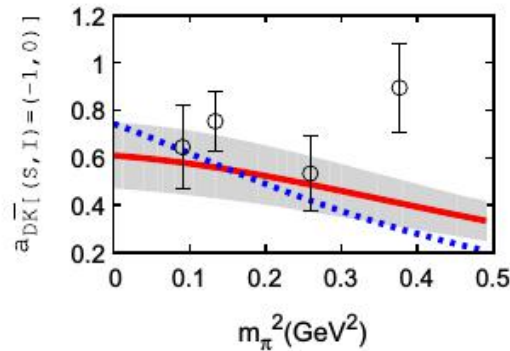
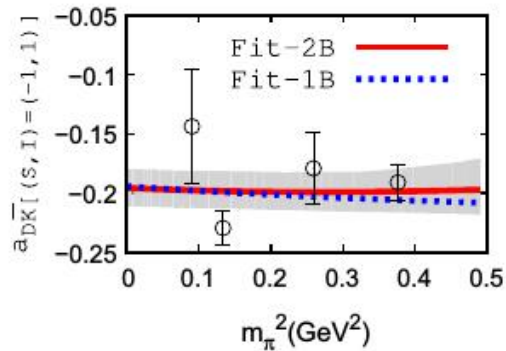


D-pi, D-eta, Ds-Kbar scattering and D*₀(2400)

Reproduction of lattice scattering lengths

[L.Liu,Orginos,F.K.Guo,Meissner, PRD'13]

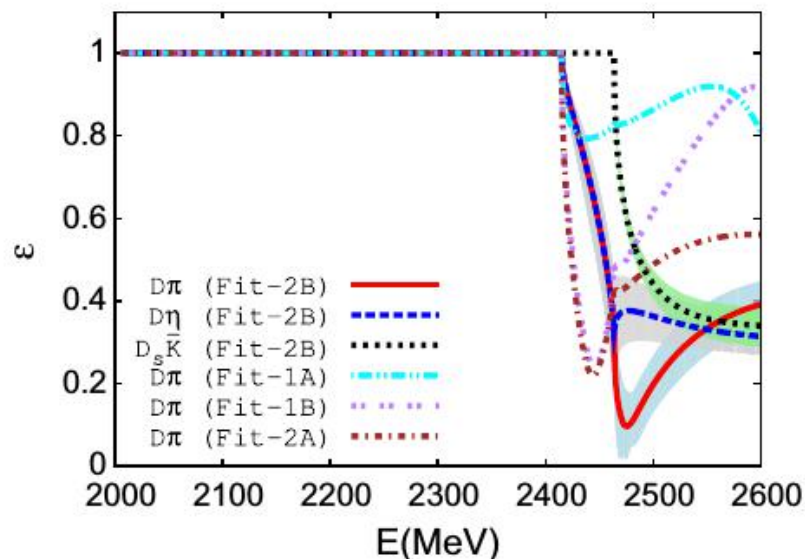
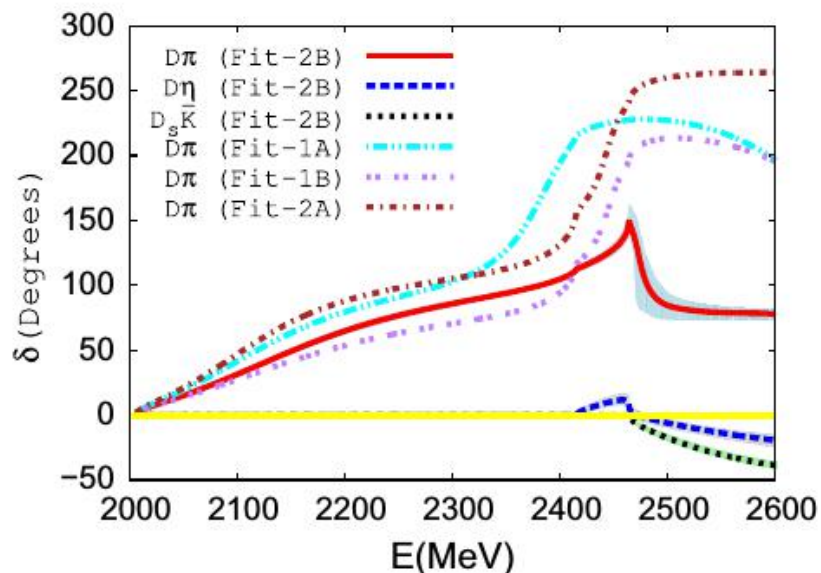
[Lang,Leskovec,Mohler,Prelovsek,Woloshyn,PRD'14]



D-pi, D-eta, Ds-Kbar scattering and D*₀(2400)

Prediction of the D-pi phase shifts and inelasticities at physical masses

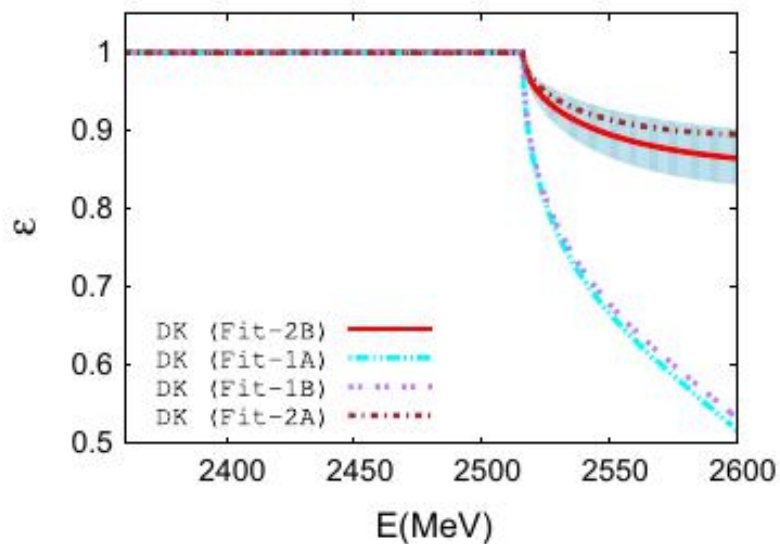
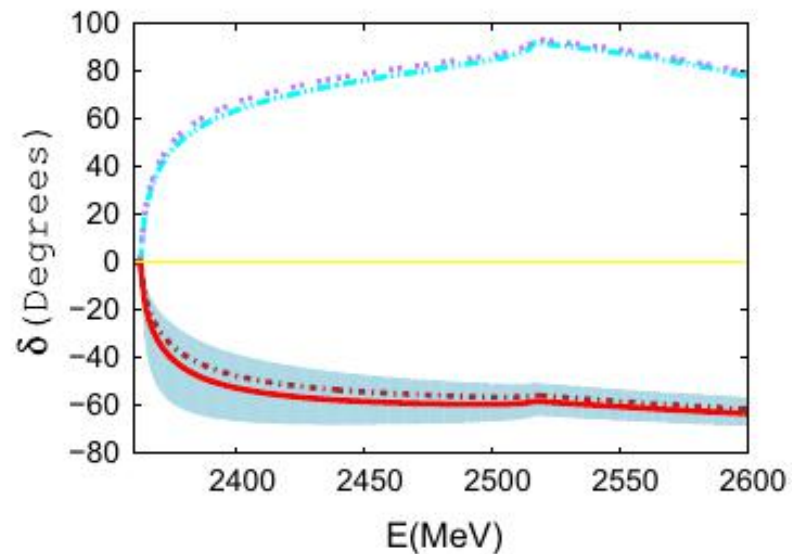
[ZHG, Liu, Meissner, Oller, Rusetsky, EPJC'19]



Poles and residues

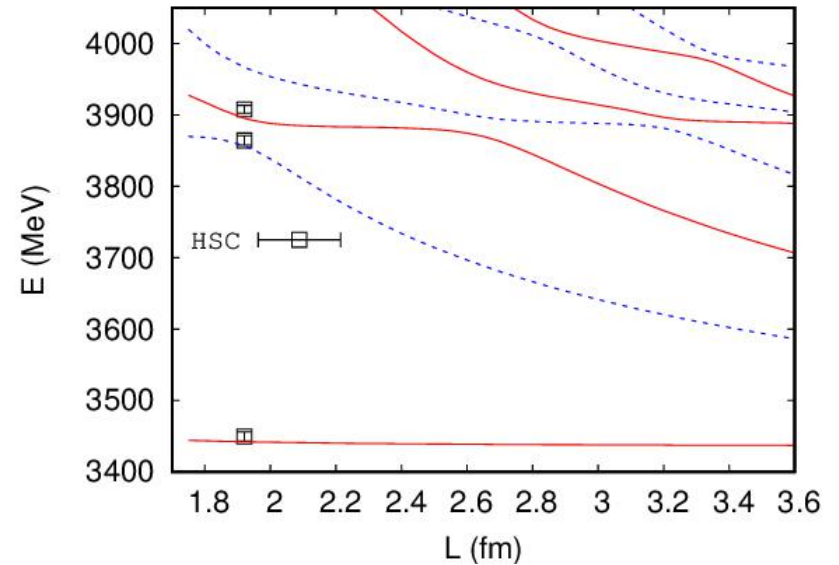
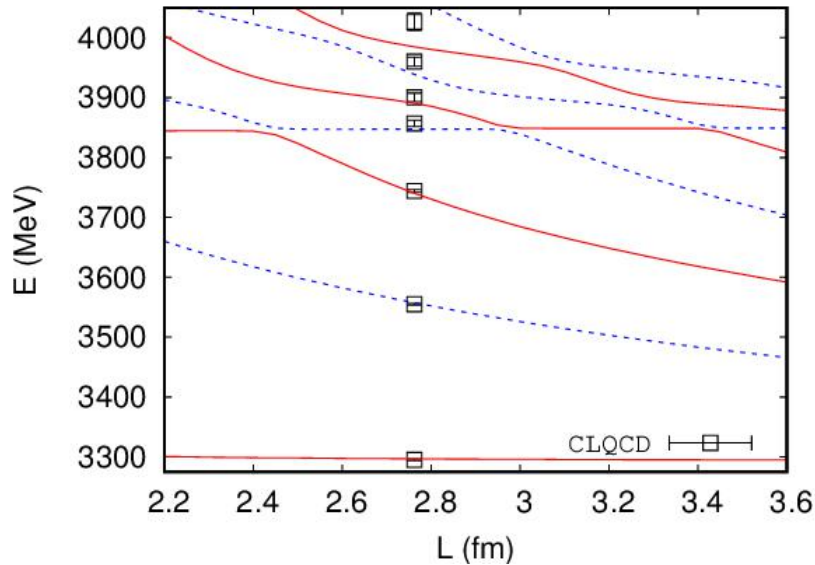
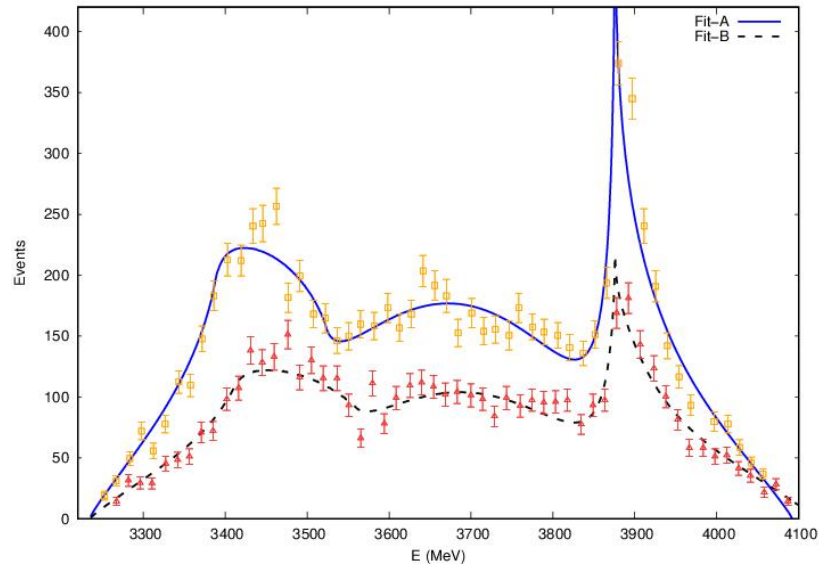
Fit	RS	M	$\Gamma/2$ (MeV)	$ \gamma_1 $ (GeV)	$ \gamma_2/\gamma_1 $	$ \gamma_3/\gamma_1 $
Fit-1A	II	$2097.7^{+6.8}_{-6.1}$	$112.2^{+16.5}_{-14.2}$	$9.6^{+0.3}_{-0.3}$	$0.10^{+0.05}_{-0.04}$	$0.78^{+0.08}_{-0.08}$
Fit-1A	II	$2384.4^{+26.4}_{-23.6}$	$36.0^{+9.9}_{-10.0}$	$4.8^{+0.5}_{-0.6}$	$1.51^{+0.15}_{-0.16}$	$2.09^{+0.18}_{-0.18}$
Fit-1B	II	$2106.4^{+5.1}_{-5.0}$	$170.6^{+12.5}_{-13.0}$	$10.1^{+0.3}_{-0.2}$	$0.11^{+0.07}_{-0.07}$	$0.79^{+0.07}_{-0.07}$
Fit-1B	III	$2409.0^{+22.7}_{-24.5}$	$78.6^{+20.5}_{-15.2}$	$6.1^{+0.7}_{-0.6}$	$1.22^{+0.19}_{-0.19}$	$2.72^{+0.48}_{-0.49}$
Fit-2A	II	$2095.7^{+5.2}_{-6.8}$	$97.1^{+10.3}_{-10.7}$	$9.4^{+0.2}_{-0.2}$	$0.10^{+0.02}_{-0.02}$	$0.63^{+0.03}_{-0.03}$
Fit-2A	III	$2401.3^{+20.4}_{-19.6}$	$55.0^{+14.5}_{-10.8}$	$5.1^{+0.5}_{-0.5}$	$1.31^{+0.19}_{-0.15}$	$2.50^{+0.31}_{-0.28}$
Fit-2B	II	$2117.7^{+3.8}_{-3.4}$	$145.0^{+8.0}_{-6.8}$	$10.2^{+0.2}_{-0.1}$	$0.09^{+0.03}_{-0.03}$	$0.58^{+0.04}_{-0.03}$
Fit-2B	III	$2470.5^{+25.1}_{-24.9}$	$104.1^{+16.0}_{-12.5}$	$6.7^{+0.7}_{-0.6}$	$1.14^{+0.12}_{-0.12}$	$2.06^{+0.16}_{-0.16}$

D-K, Ds-eta scattering and $D_{s0}^*(2317)$



Fit	RS	M (MeV)	$\Gamma/2$ (MeV)	$ \gamma_1 $ (GeV)	$ \gamma_2/\gamma_1 $
Fit-1A	I	2356.7–2362.8	0	1.3–6.9	1.03–1.20
Fit-1A	II	2316.7–2362.8	0	0.4–10.1	1.14–1.50
Fit-1B	I	2357.1–2362.8	0	0.5–6.7	1.05–1.22
Fit-1B	II	2316.0–2362.8	0	0.6–10.3	1.12–1.56
Fit-2A	I	$2345.1^{+14.7}_{-41.5}$	0	$8.3^{+2.3}_{-2.6}$	$0.96^{+0.06}_{-0.08}$
Fit-2B	I	$2350.7^{+9.0}_{-25.7}$	0	$7.7^{+2.1}_{-2.0}$	$0.83^{+0.08}_{-0.06}$

J/psi- π DD* scattering and $Z_c(3900)$ [ZHG, et al., in preparation]



Lattice data : [T.Chen, et al., (CLQCD), '19CPC] [Cheung, et al., (HSC), '17JHEP]

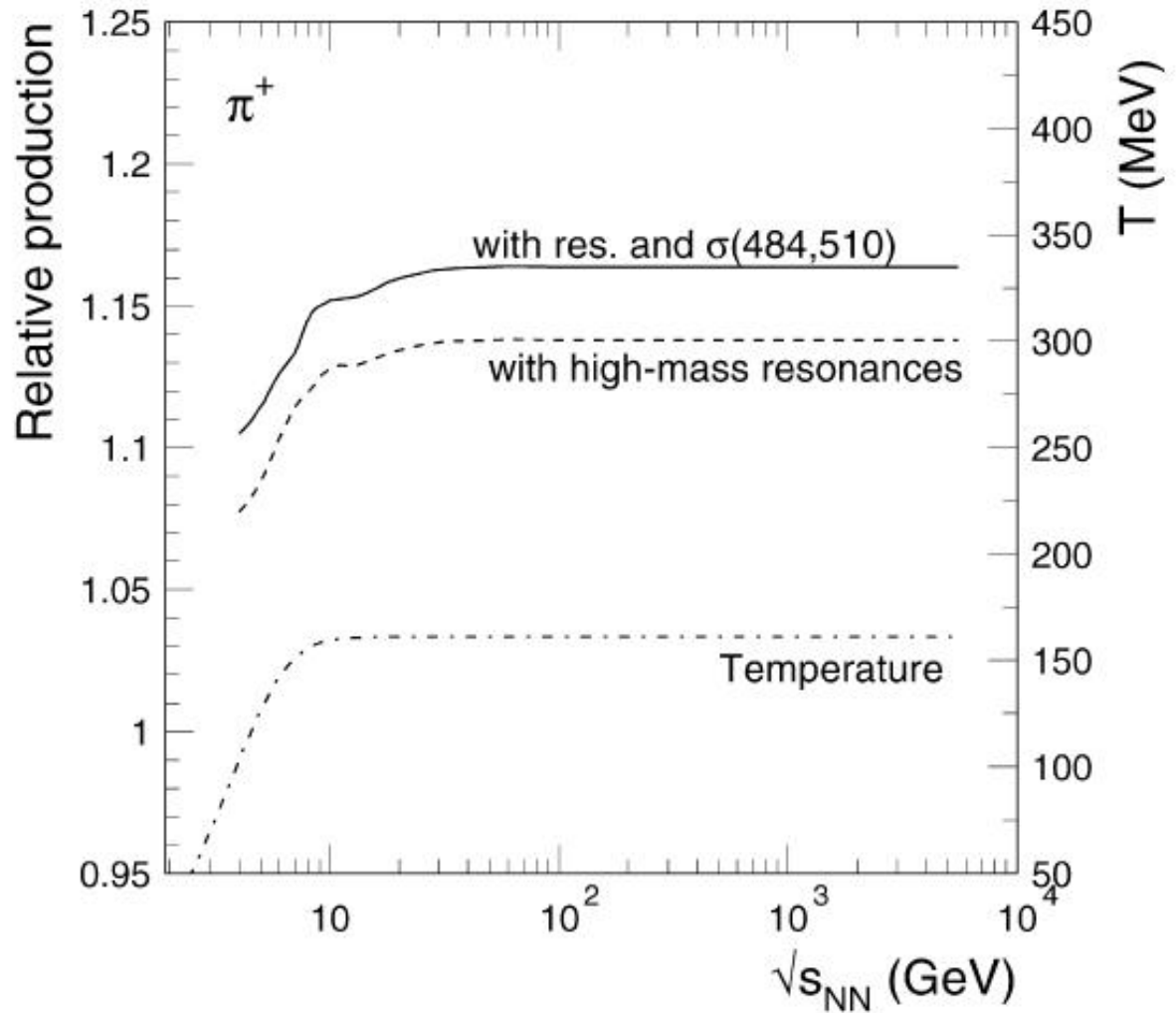
Scalar resonance at finite temperatures

Importance of the broad scalar sigma resonance: to improve the description of the hadron yields

[Andronic, Braun-Munzinger, Stachel, PLB'09]

Problem:

Breit-Wigner formula unsuitable for such a broad resonance !



Finite temperature effects in unitarized chiral amplitudes

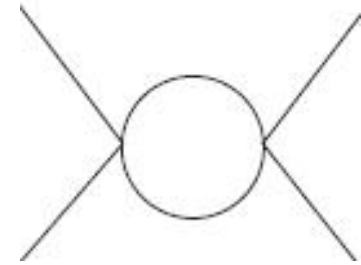
$$T_J(s) = \frac{N(s)}{1 + G(s) N(s)}$$

➤ Temperatures can enter via the $G(s)$

$$G(s) = i \int \frac{d^4 q}{(2\pi)^4} \frac{1}{(q^2 - m_1^2)[(P - q)^2 - m_2^2]}$$
$$= i \int \frac{d^3 \vec{q}}{(2\pi)^3} \int \frac{dq_0}{2\pi} \frac{1}{q_0^2 - E_1^2} \frac{1}{(P_0 - q_0)^2 - E_2^2}$$

$$q_0 \rightarrow i\omega_n = i2\pi nT, \quad dq_0 \rightarrow i2\pi T$$

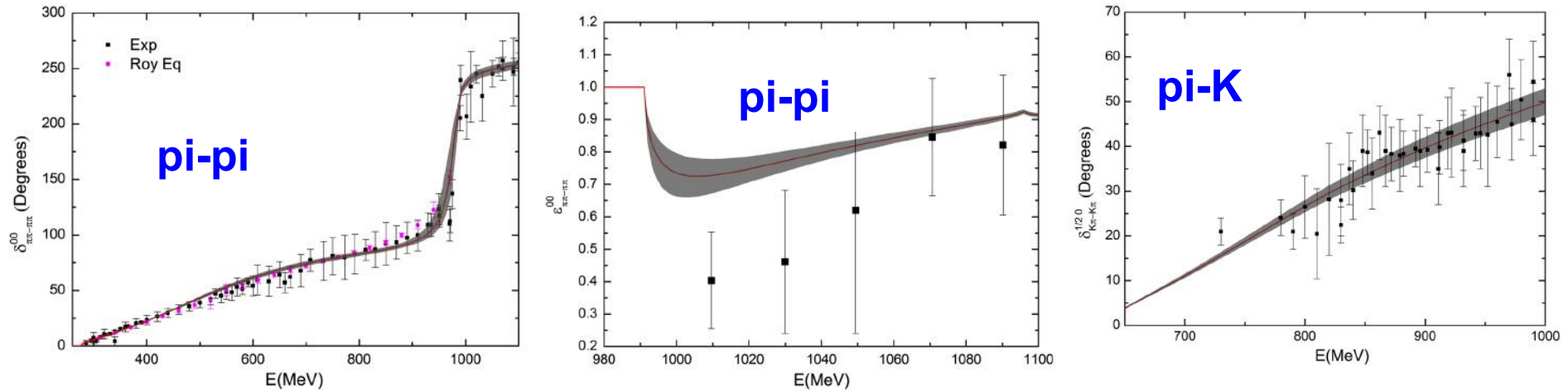
$$= \int \frac{d^3 \vec{q}}{(2\pi)^3} \sum_{n=-\infty}^{n=+\infty} T \frac{1}{\omega_n^2 + E_1^2} \frac{1}{(P_0 - i\omega_n)^2 - E_2^2}$$



Standard Matsubara techniques to calculate $G(s)$.

Be careful about the complex extrapolation !

Fits to Exp observables at zero temperature

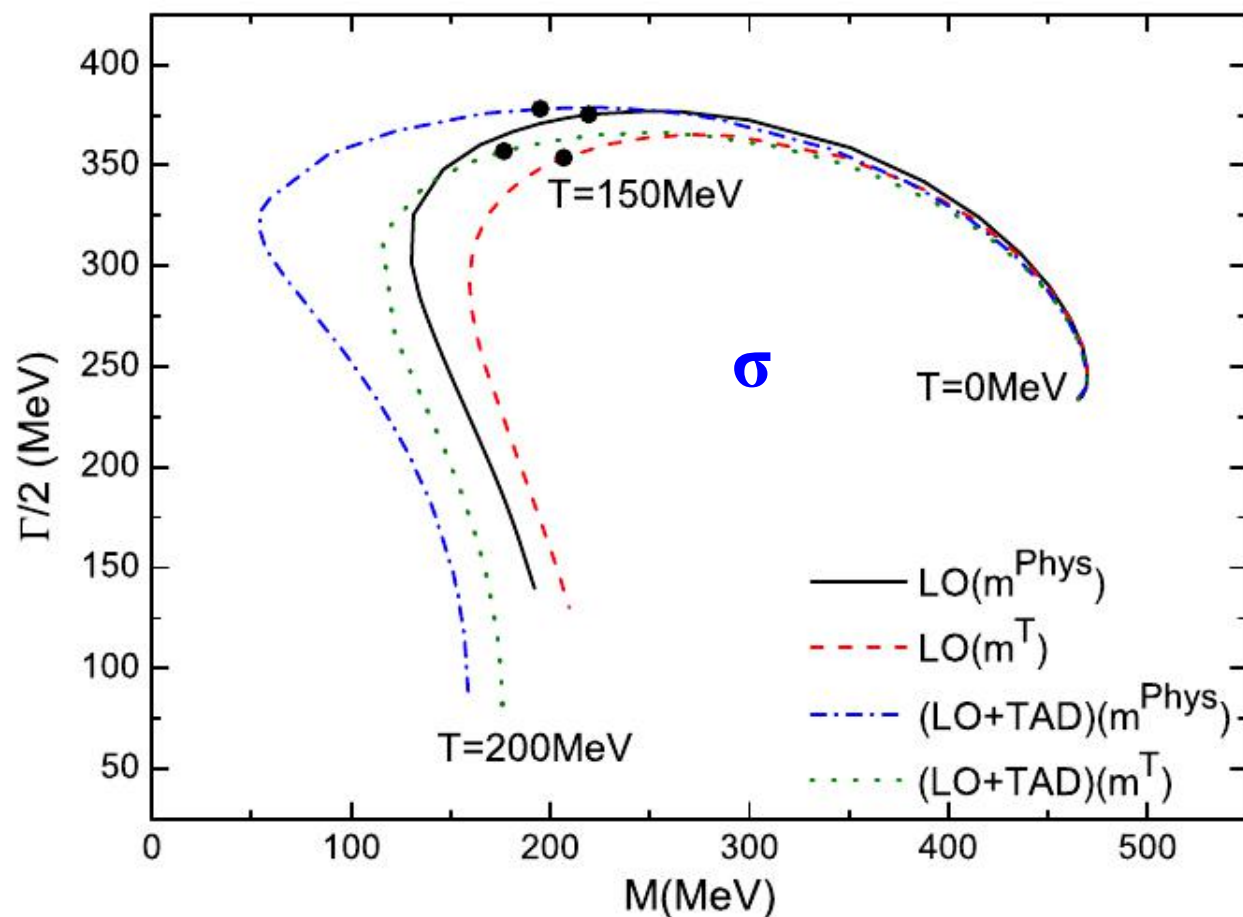


Poles and residues at zero temperature

R	$M(\text{MeV})$	$\text{Width}/2(\text{MeV})$	$ \gamma_1 \text{ (GeV)}$	Ratios	
σ	465_{-2}^{+1}	234_{-8}^{+8}	$3.14_{-0.03}^{+0.03}$	$0.45_{-0.01}^{+0.01} (K\bar{K}/\pi\pi)$ $0.067_{-0.007}^{+0.007} (\eta\eta'/\pi\pi)$	$0.02_{-0.01}^{+0.02} (\eta\eta'/\pi\pi)$ $0.06_{-0.02}^{+0.01} (\eta'\eta'/\pi\pi)$
$f_0(980)$	977_{-9}^{+6}	15_{-3}^{+5}	$1.29_{-0.15}^{+0.19}$	$3.05_{-0.57}^{+0.64} (K\bar{K}/\pi\pi)$ $1.06_{-0.19}^{+0.20} (\eta\eta'/\pi\pi)$	$2.23_{-0.47}^{+0.56} (\eta\eta'/\pi\pi)$ $1.10_{-0.21}^{+0.24} (\eta'\eta'/\pi\pi)$
κ	738_{-9}^{+8}	274_{-9}^{+8}	$4.22_{-0.07}^{+0.06}$	$0.46_{-0.02}^{+0.02} (K\eta/K\pi)$	$0.39_{-0.02}^{+0.01} (K\eta'/K\pi)$
$a_0(980)$	1037_{-14}^{+17}	44_{-9}^{+6}	$3.8_{-0.2}^{+0.3}$	$1.43_{-0.03}^{+0.03} (K\bar{K}/\pi\eta)$	$0.05_{-0.01}^{+0.01} (\pi\eta'/\pi\eta)$

Prediction of the trajectories of sigma resonance when increasing temperatures

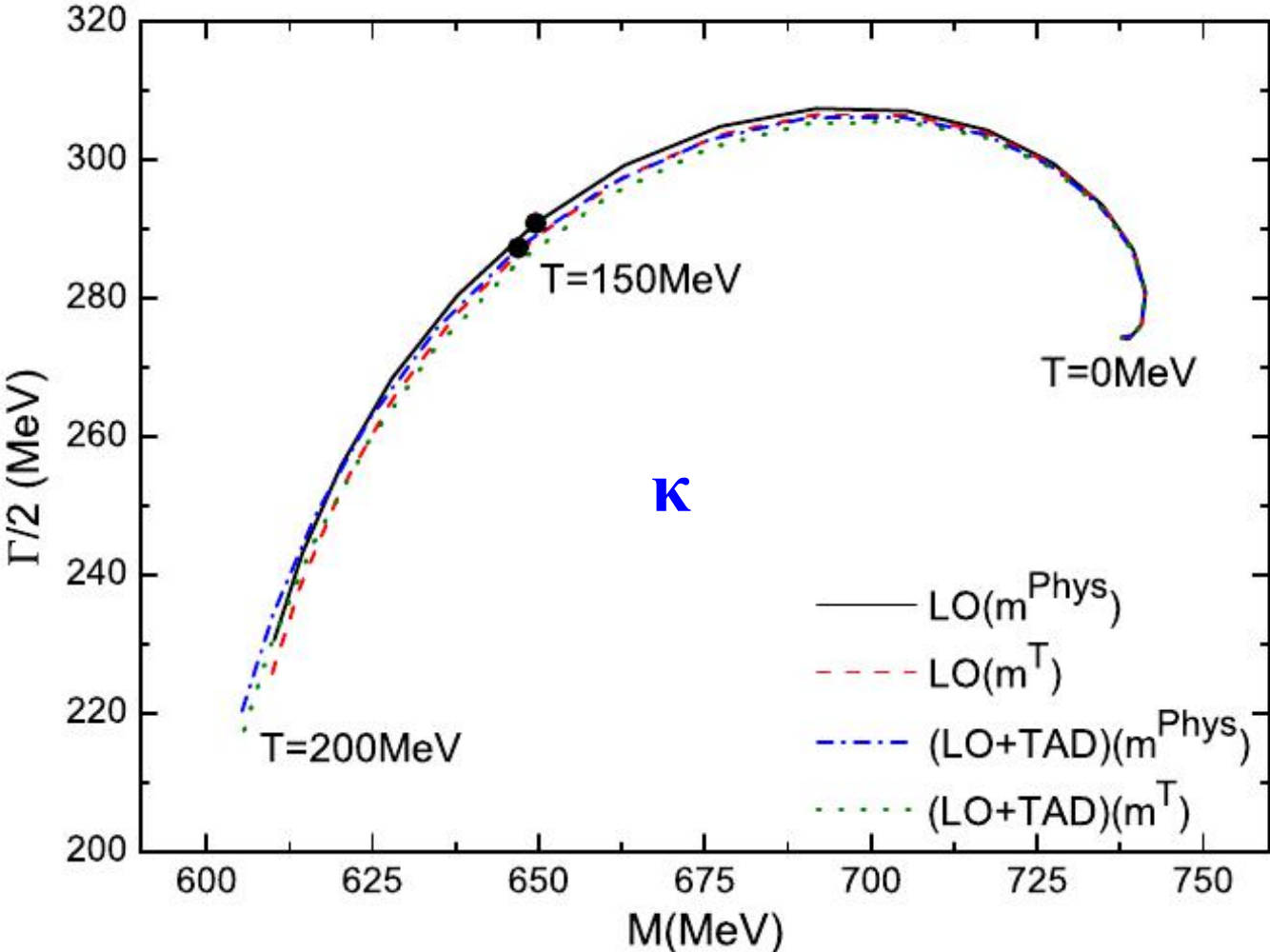
[Gao, ZHG, Pang, PRD'19]

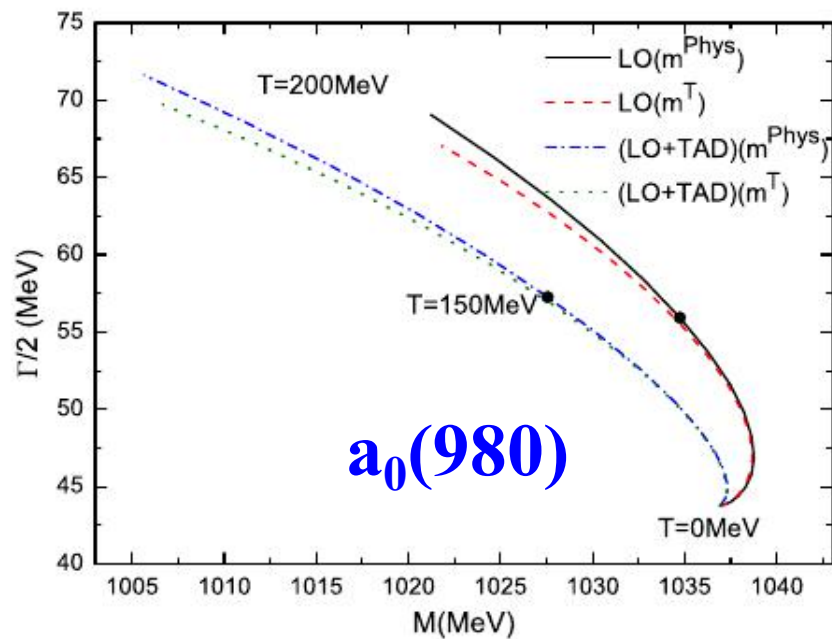
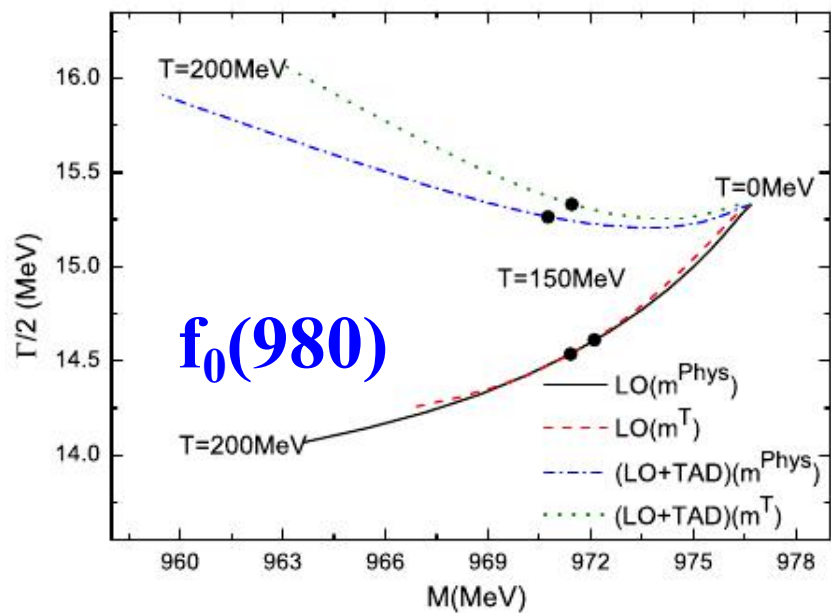


➤ It would be very interesting for our lattice colleagues to calculate the pi-pi scattering at finite temperatures

Kappa resonance at finite temperatures

[Gao, ZHG, Pang, PRD'19]





[Gao, ZHG, Pang, PRD'19]

Conclusions

- **The chiral approach illustrated in this talk provides an efficient way to study the finite-volume energy levels.**
- **It can build a bridge to connect the lattice eigenenergies in finite box obtained at unphysical masses with the physical observables, such as phase shifts, inelasticities, at physical meson masses.**
- **It is rather encouraging for the lattice community to calculate the scattering processes at finite temperatures! So one can trace the finite-temperature trends of the physical resonances, instead of the toy ones!**

Thanks for your attention!